DEUTSCHES ELEKTRONEN-SYNCHROTRON DESY

DESY 72/36
April 1972

Polarization Effects in Deep Inelastic Lepton-Nucleon Scattering

by

T.F. Walsh

II. Institut für Theoretische Physik der Unuversität Hamburg

and

P. Zerwas

Deutsches Elektronen-Synchrotron DESY, Hamburg

2 HAMBURG 52 · NOTKESTIEG 1

Polarization Effects in Deep Inelastic Lepton - Nucleon Scattering

by

T. F. Walsh

II. Institut für Theoretische Physik der Universität Hamburg

and

P. Zerwas[+]

Deutsches Elektronen-Synchrotron DESY, Hamburg

[+]On leave from III. Physikalisches Institut der Technischen Hochschule Aachen.

Abstract:

In this report we give an introduction to questions related to polarization experiments in deep inelastic lepton-nucleon scattering. After discussing the kinematics we present a summary of the results from different models which have been proposed as descriptions of spin effects in the Bjorken scaling region. We estimate longitudinal and perpendicular asymmetries at various incident lepton energies and scattering angles in order to show how to distinguish between models which give nearly identical results for spin averaged cross sections.

Introduction

Deep inelastic scattering of unpolarized electrons on unpolarized proton and deuteron targets has been a field of intense activity in the last few years. Experimentally, a 'scaling' behavior |1| is suggested over a very wide kinematical range |2|: for momentum transfers $|Q^2| \gtrsim 0.5$ GeV^2 and CM energies of the virtual photon-nucleon system $W \gtrsim 2$ GeV. Roughly three theoretical pictures have emerged—two intuitive and one more abstract in nature. The first one, Feynman's parton model, assumes that in the CM system of the electron and nucleon the target appears to be a set of free constituents which scatter incoherently |3-6|. In the second, the scaling behavior is assumed to arise as a result of a collective and coherent process: the excitation of asymptotically many overlapping nucleon resonances |7|. The third picture is based on the more abstract light cone analysis, in which the scaling behavior is taken to yield information on the structure of the commutator of the electromagnetic current with itself near the light cone in configuration space |8,9,6|.

These models, and (probably) those to be expected in the near future, have the common property that they do not determine the functional form of the scaling functions $F_1(\omega)$ and $F_2(\omega)$, which enter the cross section from first principles alone. All models can be expected to involve unknown parameters which are adjusted to fit the data. The extreme case is the light cone analysis, in which the functional form of F_1 and F_2 is unknown except for some constraints in the form of sum rules. It is clear that decisive tests of such models cannot follow from measurements of the spin averaged deep inelastic scattering alone. That measurement of this cross section alone is insufficient to give detailed tests of models beyond checking the validity of the familiar sum rules is also clear from the naive observation that cross sections often only contain information about gross properties of physical processes. In order to make further progress in understanding the physical processes underlying the scaling phenomenon, one has to turn to quantities which are more sensitively dependent on the physical structure of the various models than the spin averaged cross sections or, equivalently, the structure functions F_1 and F_2. The quantities of interest in this connection are the two spin-dependent structure functions of the nucleon, which average to zero when one studies spin-averaged inelastic electron-nucleon scattering |10-17|.

Deep inelastic scattering to date has corresponded to the measurement of total cross sections for virtual photons with a partial linear polarization. Measurement of polarization asymmetries will mean that one has the

additional advantage of having a circularly polarized virtual photon. In the spin averaged case, the linear polarization components of the virtual photon are added together incoherently. With a polarized lepton beam, on the contrary, these components of the virtual photon are coherent.

A parallel worth mentioning at this point is the relation of measurements of differential cross sections for $\pi^- p \to \pi^0 n$, measurements of the polarization P in this reaction, and the Regge models for the process. It is well known that measurements of the spin averaged cross section $d\sigma/dt$ are insufficient to constrain the Regge fits to $\pi^- p \to \pi^0 n$. In order to discriminate different models, one has to measure the polarization P. These measurements have had a decisive influence on the growth of Regge pole theory and, one hopes, of the general understanding of hadron-hadron scattering. The parallel is inexact, as the study of inelastic electron nucleon scattering till now has not yet reached a very detailed level, but it can be expected that measurements of the spin-dependent effects in this process are as important for understanding as are the measurements of spin-dependent effects in the example we have just mentioned.

The report is organized as follows. We discuss the kinematics in the next Section I and the scaling behavior and specific models in the following Section II. In the last Section III we give a summary of the results so far obtained, and finally an Appendix containing some useful formulas and a list of various authors' conventions and definitions together with the relations between the different conventions. A series of figures can be found at the end of the report. They, together with their captions, are designed to be independently intelligible. We have chosen to give asymmetries for beam energies 5 GeV (DESY), 15 GeV (SLAC), 50 GeV, 100 GeV (CERN II, Batavia).

I. Kinematics

1. The inclusive reaction $\ell(\vec{k},\beta) + N(p,\alpha) \to \ell'(k',\beta') + \text{hadrons}$ is described in lowest order electromagnetism by one-photon exchange [Fig. 1].

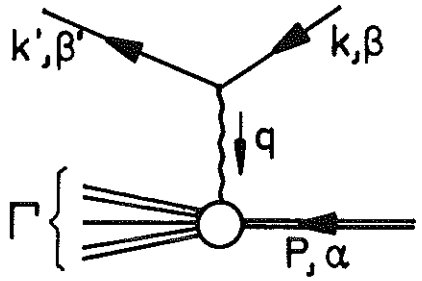

Fig. 1

$q = k - k'$ is the 4-momentum of the virtual photon and β, β' are the polarization four-vectors of the in- and outgoing leptons (we assume μ- e universality and refer to 'electrons' in what follows), and α denotes the nucleon polarization vector. These are spacelike pseudovectors, orthogonal to the respective momenta. In the particle rest frame they have only space components whose length is put equal to the mass of the particle. Otherwise ignoring the lepton mass, we have in the laboratory frame with the 1-3 plane as the scattering plane [Fig. 2].

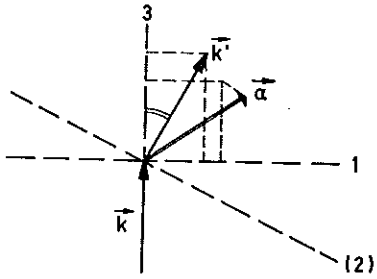

Fig. 2

$$k = (E, 0, 0, E)$$
$$k' = (E', E'\sin\Theta, 0, E'\cos\Theta)$$
$$\alpha = (0, \alpha_\perp, \alpha_N, \alpha_\parallel)$$

where $\alpha_\parallel$ denotes the polarization component parallel to the incident electron momentum, $\alpha_\perp$ the perpendicular component lying in the electron scattering plane and α_N that component which is normal to this plane. We remark that the leptons have to be longitudinally polarized, as transverse lepton polarization leads to effects porportional to the electron mass.

The T matrix element |*| for producing a hadron system Γ is

$$T = e^2\, \bar{u}\,(k'\beta')\gamma^\mu\ u(k,\beta)\ \frac{1}{q^2} < \Gamma\ ;\ \text{out}\ |I_\mu|\ p,\alpha >$$

|*| We define $S = 1 + i(2\pi)^4\, \delta_4(\Sigma p)T$; states and spinors are normalized as $<A|B> = (2\pi)^3\, 2E\, \delta_{S_A S_B}\, \delta_3(\vec{p}_A - \vec{p}_B)$ and $\bar{u}\, u = 2\, m$, respectively.

and we obtain the total cross section

$$d^3\sigma_{\alpha\beta} = \frac{\alpha^2}{(q^2)^2 \sqrt{(k\cdot p)^2}} \frac{d^3k'}{E'} \mathbb{L}^{\mu\nu}(\beta) \mathbb{W}_{\mu\nu}(\alpha) \qquad (1)$$

where $\mathbb{L}^{\mu\nu}(\beta)$ is the electron tensor and $\mathbb{W}_{\mu\nu}(\alpha)$ the (spin-dependent) hadron tensor. This factorization is the nice property of one-photon exchange. We can write the electron tensor as the sum of a spin averaged symmetric piece and an antisymmetric piece which alone contains the explicit spin effects of $\mathbb{L}^{\mu\nu}$.

$$\mathbb{L}^{\mu\nu}(\beta) = \frac{1}{2} L^{\mu\nu} + \frac{i}{2} A^{\mu\nu}(\beta)$$

$$L^{\mu\nu} = 4(k^\mu k'^\nu + k^\nu k'^\mu + \frac{1}{2} q^2 g^{\mu\nu}) \qquad (2)$$

$$A^{\mu\nu} = 4\, \varepsilon^{\mu\nu\rho\sigma} q_\rho \beta_\sigma$$

In the same way, we decompose the hadron tensor into a symmetric piece and an antisymmetric piece under exchange $\alpha \leftrightarrow -\alpha$:

$$\mathbb{W}^{\mu\nu}(\alpha) = W^{\mu\nu} + i X^{\mu\nu}(\alpha)$$

$$W^{\mu\nu} = \frac{1}{4\pi} \int d^4x\, e^{iq\cdot x} \frac{1}{2} \{\langle p,\alpha|[I_\mu(x), I_\nu(o)]\,|\,p,\alpha\rangle$$

$$+ \langle p,-\alpha|\,[I_\mu(x), I_\nu(o)]\,|p,-\alpha\rangle\} \qquad (3)$$

$$iX^{\mu\nu} = \frac{1}{4\pi} \int d^4x\, e^{iqx} \frac{1}{2} \{\langle p,\alpha|\,[I_\mu(x), I_\nu(o)]\,|p,\alpha\rangle$$

$$- \langle p,-\alpha|\,[I_\mu(x), I_\mu(o)]\,|p,-\alpha\rangle\}$$

The tensors $L^{\mu\nu}$ and $W^{\mu\nu}$ are already familiar from the spin average case.

2. We are now in a position to write the cross section in terms of the unpolarized cross section and the asymmetry, defined as [14]

$$d\sigma_{\alpha\beta} = d\sigma_{unpol}\,[\,1 + \Delta_{\alpha\beta}\,]$$

$$d\sigma_{unpol} = \frac{\alpha^2}{2(q^2)^2\sqrt{(p\cdot k)^2}}\,\frac{d^3k'}{E'}\,L^{\mu\nu}W^{\mu\nu} \qquad (4)$$

$$\Delta_{\alpha\beta} = -\,\frac{L^{\mu\nu}\,Im\,X_{\mu\nu}(\alpha) + A^{\mu\nu}(\beta)\,Im\,W_{\mu\nu} + A^{\mu\nu}(\beta)\,Re\,X_{\mu\nu}(\alpha)}{L^{\mu\nu}\;W_{\mu\nu}}$$

By the hermiticity of the electromagnetic current and invariance under parity transformations, which we assume from now on, $Im\,W_{\mu\nu} = 0$. Since in the laboratory system $\Delta_{\alpha\beta}$ has then to be linear in $\vec{\alpha}$, we have three independent asymmetry components for $\vec{\beta}$ parallel to $\vec{k}$, namely

$$\Delta_{\alpha\beta} = \vec{\Delta}\cdot\vec{\alpha} \qquad \text{with} \qquad \begin{aligned}\Delta^3 &\equiv \Delta_{\parallel}\\ \Delta^1 &\equiv \Delta_{\perp}\\ \Delta^2 &\equiv \Delta_N\end{aligned} \qquad (5)$$

We see now that one has to carry out three experiments to get all the available dynamical information. However, we can assume time reversal invariance for the strong and electromagnetic interactions so as to eliminate $\Delta_N = 0$. For $\vec{\alpha}$ perpendicular to the scattering plane [Fig. 3a.] we have listed the nonvanishing expressions in Table 1 together with their transformation properties under P and T. Clearly, there exists no T invariant term corresponding to $\Delta_N \neq 0$. We note that the vanishing of Δ_N is not, however, a sufficient condition for T invariance to hold. Restricting ourselves to $\Delta_{||}$ and $\Delta_{\perp}$, the parallel and vertical asymmetries, which one must measure assuming P and T invariance, we give experimental configurations in Fig. 3b. and 3 c.

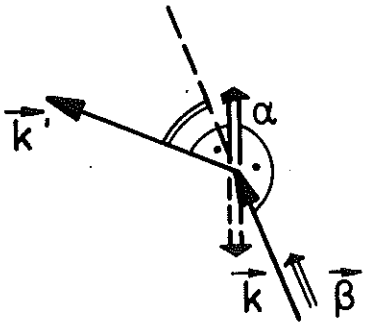

Fig. 3a

$\Delta_N \sim$	P	T
$\vec{\alpha}(\vec{k}\times\vec{k}')$	O.K.	X
$\vec{\alpha}(\vec{\beta}\times\vec{k}')$	X	X

Table 1.

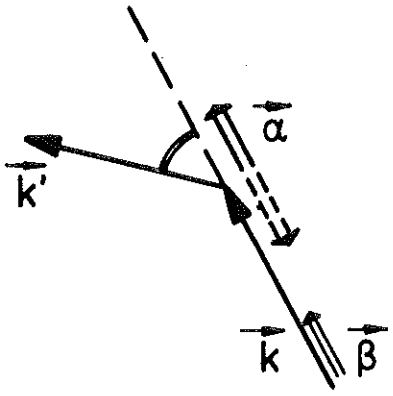

Fig. 3b

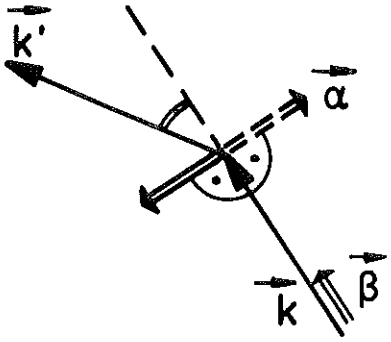

Fig. 3c

3. Using P and T invariance, we can write for W or the full Compton amplitude T a decomposition in terms of the helicity amplitudes in the s-channel for forward off-shell Compton scattering. We have four independent amplitudes

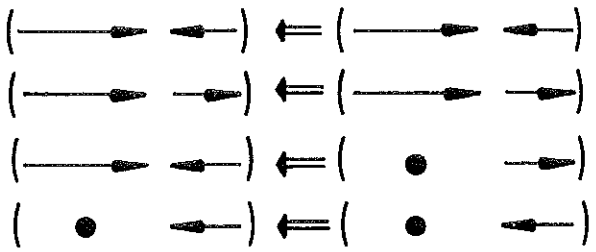

$f^S_{1\,1/2\,\leftarrow\,1\,1/2}$

$f^S_{1\,-1/2\,\leftarrow\,1\,-\,1/2}$

$f^S_{0\;1/2\,\leftarrow\,0\;1/2}$

$f^S_{0\,-1/2\,\leftarrow\,1\;1/2}$

where the helicities are as follows: " $\rightleftharpoons$ " $\cdot\cdot\lambda_\gamma = \pm 1$, " $\bullet$ " $\cdot\cdot\lambda_\gamma = 0$ and ' $\rightleftarrows$ ' $\cdot\cdot\lambda_N = \pm\, 1/2$. Therefore, we have four independent functions in the invariant decomposition of W , which we choose as follows

$$W^{\mu\nu} = \left(- g^{\mu\nu} + \frac{q^\mu q^\nu}{q^2} \right) W_1(\nu,q^2) + \left(p^\mu - \frac{p\cdot q}{q^2} q^\mu\right)\left(p^\nu - \frac{p\cdot q}{q^2} q^\nu\right) W_2(\nu,q^2)$$

(6)

$$X^{\mu\nu} = \varepsilon^{\mu\nu\lambda\sigma}\, q_\lambda \alpha_\sigma\, X_1(\nu,q^2) + (\alpha\cdot q)\varepsilon^{\mu\nu\lambda\sigma}\, q_\lambda p_\sigma\, X_2(\nu,q^2)$$

and where we have defined $\nu = p \cdot q$. The symmetry of $W^{\mu\nu}$ and antisymmetry of $X^{\mu\nu}$ are consequences of PT invariance; the hermiticity of $I_\mu(x)$ requires then $X^{\mu\nu}$ and $W^{\mu\nu}$ real. Necessarily, both target and beam must be polarized in order to get an effect, or else one has to measure the final lepton polarization with a polarized target and unpolarized beam.

4. Having discussed the discrete symmetries and the invariant amplitudes, we now turn to crossing and to constraints from the positivity of the tensor $W^{\mu\nu}$, $a^*_\mu W^{\mu\nu} a_\nu \geq 0$ for arbitrary complex vector a. From crossing,

$$\begin{aligned} W_{1,2}\,(-\nu,q^2) &= -\,W_{1,2}\,(\nu,q^2) \\ X_1\,(-\nu,q^2) &= -\,X_1\,(\nu,q^2) \\ X_2\,(-\nu,q^2) &= +\,X_2(\nu,q^2). \end{aligned} \tag{7}$$

From positivity we get four constraints |11|,

$$\begin{aligned} &(1)\quad 0 \leq W_L\,(\nu,q^2) \\ &(2)\quad 0 \leq W_T\,(\nu,q^2) \\ &(3)\quad 0 \leq (-q^2)\,M^2\,[X_1(\nu,q^2)\,]^2 \leq W_L\,(\nu,q^2)\,W_T\,(\nu,q^2) \\ &(4)\quad 0 \leq |\nu X_1\,(\nu,q^2) + (\nu^2 - q^2M^2)\,X_2\,(\nu,q^2)\,| \leq W_T\,(\nu,q^2) \end{aligned} \tag{8}$$

The first two constraints are just that the familiar transverse and longitudinal virtual photon cross sections σ_T and σ_L satisfy $\sigma_{T,L} \geq 0$ since $\sigma_T \sim W_T$ and $\sigma_L \sim W_L$, where

$$\begin{aligned} W_T &\equiv W_1 \\ W_L &\equiv (M^2 - \nu^2/q^2)\,W_2 - W_1 \end{aligned} \tag{9}$$

The second two constraints arise from the condition that the asymmetries be ≤ 1 - again a condition from positivity of cross sections. We define (see the Appendix) the cross sections σ_T and σ_L as porportional to the absorptive parts of the corresponding helicity amplitudes

$$\sigma_T = C\,\frac{1}{2}\,\mathrm{Im}\,[\,f_{1\ 1/2,\ 1\ 1/2} + f_{1-1/2,1-1/2}\,]$$

$$\sigma_L = C\,\mathrm{Im}\,f_{0\ 1/2,0\ 1/2}$$

Then we can write corresponding relations for the τ as

$$\tau_T = C \frac{1}{2} \mathrm{Im} \left[f_{1\ 1/2,\ 1\ 1/2} - f_{1-1/2,1-1/2} \right]$$

$$\tau_L = C\ \mathrm{Im}\ f_{1\ 1/2,\ 0-1/2}$$

The proportionality coefficients are irrelevant to the positivity conditions,

$$\begin{aligned} &(1)\ 0 \leq \sigma_L \\ &(2)\ 0 \leq \sigma_T \\ &(3)\ 0 \leq (\tau_L)^2 \leq 2\ \sigma_L \sigma_T \\ &(4)\ 0 \leq (\tau_T)^2 \leq (\sigma_T)^2, \end{aligned} \tag{10}$$

from which the origin of the inequalities becomes obvious.

The third constraint equation provides an interesting lower limit of the longitudinal cross section σ_L, once τ_L or $X_1^{\ 2}$ is measured. Anticipating for the moment the model dependent light cone algebra result $X_1 \to \nu^{-1}$, we see that W_L cannot vanish faster than $(-q^2)/\nu^2$ |*|.

We conclude this section by summarizing the properties of the asymmetries $\Delta_{||}$ and $\Delta_{\perp}$. In terms of laboratory variables,

$$\begin{aligned} \Delta_{||} &= \frac{d\sigma(\uparrow\downarrow) - d\sigma(\uparrow\uparrow)}{d\sigma(\uparrow\downarrow) + d\sigma(\uparrow\uparrow)} = \\ &= \frac{M(E+E'\cos\Theta)\ X_1(\nu,q^2) + M^2(E+E')(E-E'\cos\Theta)X_2(\nu,q^2)}{W_1(\nu,q^2) + \frac{1}{2}\cot^2\theta/2\ M^2 W_2(\nu,q^2)} \end{aligned} \tag{11}$$

|*| The physical interpretation of τ_L is obscure because it is related to a helicity amplitude with one off-shell longitudinal and one transverse photon. It vanishes at least as fast as $\sqrt{-q^2}$ as $-q^2 \to 0$ (see the Appendix). In contrast, τ_T can be measured at $q^2 = 0$ from the total photoabsorption cross section of a circularly polarized photon scattered on a polarized target. Note, that $\tau_L(q^2=0)$ appears in the Drell-Hearn-Gerasimow sum rule

$\int_0^\infty \frac{d\nu}{\nu} [\sigma_{\uparrow\uparrow}(\nu,q^2=0) - \sigma_{\uparrow\downarrow}(\nu,q^2=0)] = \frac{2\pi^2\alpha}{M^2} \mu_p^{\ 2}$, where μ_p is the anomalous magnetic moment of the proton in units of the nucleon magneton.

and

$$\Delta_\perp = \frac{d\sigma(\uparrow\leftarrow) - d\sigma(\uparrow\rightarrow)}{d\sigma(\uparrow\leftarrow) + d\sigma(\uparrow\rightarrow)} =$$

$$= \frac{ME'\sin\theta\,[X_1(\nu,q^2) - M(E+E')\,X_2(\nu,q^2)]}{W_1(\nu,q^2) + \frac{1}{2}\cot^2\theta/2\; M^2 W_2(\nu,q^2)} \qquad (12)$$

It is possible to separate the structure functions W_1 and W_2 by measuring the spin averaged cross section for fixed $\nu=(E-E')/M$ and $q^2 = -4EE'\sin^2\theta/2$ but with different incident energy and different angle. The same procedure for X_1, X_2 is only possible at small energies, measuring $\Delta_{||}$ with ν and q^2 fixed, since for large energies $E >> M$, this asymmetry parameter becomes |12|

$$\Delta_{||} \sim \nu\, X_1\,(\nu,q^2) + \nu^2\, X_2(\nu,q^2).$$

Since one must separate X_1 and X_2 in order to test models, the measurement of $\Delta_\perp$ is unavoidable for large energies.

The boundaries of the asymmetries following from the positivity constraints are [see |17|]

$$|\Delta_{||}| \leq \frac{\sqrt{\frac{R}{-q^2}}\left|(E+E'\cos\theta) - \frac{\nu M(E+E')}{\nu^2 - M^2q^2}(E-E'\cos\theta)\right| + \frac{M^2(E+E')}{\nu^2 - M^2q^2}(E-E'\cos\theta)}{1 + \frac{1}{2}\cot^2\frac{\theta}{2}\,\frac{1+R}{1-\frac{\nu^2}{q^2M^2}}} \qquad (13)$$

and

$$|\Delta_\perp| \leq \frac{ME'\sin\theta\left\{\sqrt{\frac{R}{-q^2M^2}}\left[1 + \frac{\nu M(E+E')}{\nu^2 - M^2q^2}\right] + \frac{M(E+E')}{\nu^2 - M^2q^2}\right\}}{1 + \frac{1}{2}\cot^2\frac{\theta}{2}\,\frac{1+R}{1-\frac{\nu^2}{q^2M^2}}} \qquad (14)$$

where $R = \sigma_L(\nu,q^2)/\sigma_T(\nu,q^2)$. These boundaries appear at the end of this report among the figures.

II. Scaling Behavior and Models.

The functions W_1 und W_2 seem to scale, in the sense that they become functions of the dimensionless variable

$$\omega = 2\nu/(-q^2) \text{ with } 1 \leq \omega \leq \infty$$

as q^2 and ν become large enough (Bjorken limit)|1,2|.The factor ν in front of W_2 is present on naive dimensional grounds:

$$\lim_{\substack{\nu,|q^2|\to\infty \\ \text{fixed}}} W_1(\nu, q^2) = F_1(\omega)$$

$$\lim_{\substack{\nu,|q^2|\to\infty \\ \omega \text{ fixed}}} \nu W_2(\nu,q^2) = F_2(\omega)$$

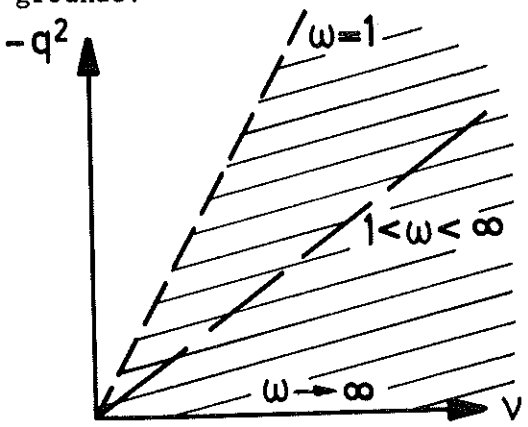

Fig. 4

The scaling functions are nonzero and the limit appears to be reached rapidly in the ν,q^2 plane, νW_2 becoming roughly constant along rays ω = constant already for $|q^2| \gtrsim 0.5$ GeV^2. We shall take this scaling behavior as established, although there may be deviations not yet apparent. We can now ask what sort of behavior for X_1 und X_2 is allowed assuming that, apart from a definite power of ν, these functions 'scale', too. From the positivity conditions, and the requirement that W_L and W_T be functions of ω alone, we find that the maximal allowed ν dependence would lead to scaling in the form

$$X_1(\nu,q^2) \to \nu^{-1/2} \text{ x (scaling function)}$$

$$X_2(\nu,q^2) \to \nu^{-3/2} \text{ x (scaling function)}$$

If, however, the longitudinal structure function W_L vanishes in the asymptotic limit a stronger decrease with ν is enforced. Naive counting of dimensions leads as well to the guess

$$X_1(\nu,q^2) \to \nu^{-1} \text{ x (scaling function)}$$

$$X_2(\nu,q^2) \to \nu^{-2} \text{ x (scaling function)}$$

which is, in fact, realized in some of the models we shall discuss now.

IIa. Quark Light Cone Algebra

1. A heuristic argument suggests that the main contributions to the Bjorken limit of $W^{\mu\nu}(\alpha)$ come from the region where the arguments of the electromagnetic currents are separated by a lightlike interval |8|. In the nucleon rest frame where $q = (q^o, 0, 0, q^3)$ we have in (3) the exponential factor

$$\exp(i\, q\cdot x) = \exp i\, [\tfrac{\nu}{M}\,(x^o - x^3) - \tfrac{M}{\omega}\, x^3 + O(\nu^{-1})]$$

and the significant contributions to the fourier integral can be expected to come from the volume where the phase in the above bracket is bounded, namely

$$|x^o - x^3| \lesssim M/\nu \text{ and } |x^3| \lesssim \omega/M$$

Because of causality, $[I_\mu(x), I_\nu(o)] = 0$ if $x^2 > 0$; the region dominating the integral in (3) is given by

$$0 \leq x^2 \lesssim 2\omega/\nu - x_\perp^2 \lesssim 1/(-q^2)$$

which collapses into the light cone as $q^2 \to -\infty$.

2. In order to get further, we need some information on the commutator near the light cone |9|. It should suffice to pick out the structures which are most singular at $x^2 = 0$, since we are assured that these will dominate $W^{\mu\nu}$ for large momenta. The obvious method to use is analogous to that which led Gell-Mann to conjecture the equal-time commutators of the weak and electromagnetic currents; one calculates the relevant commutators in the free quark model, and selects the part which is most singular on the light cone. The result for the antisymmetric part of the electromagnetic current commutator we will need is the following:

$$\begin{aligned}[I_\mu(x), I_\nu(o)] \;\hat{=}\; & -\tfrac{i}{4\pi}\,[\partial^\rho \varepsilon(x^o)\delta(x^2)]\;\varepsilon_{\mu\nu\rho\sigma} \\ \cdot\; & \tfrac{2}{3}\,\{\; \tfrac{1}{\sqrt{3}}\, I_8^{5\sigma}\,(o|x) + I_3^{5\sigma}\,(o|x) + 2\sqrt{\tfrac{2}{3}}\; I_o^{5\sigma}\,(o|x) \\ & + \tfrac{1}{\sqrt{3}}\, I_8^{5\sigma}\,(x|o) + I_3^{5\sigma}\,(x|o) + 2\sqrt{\tfrac{2}{3}}\, I_o^{5\sigma}\,(x|o)\;\}\end{aligned} \qquad (15)$$

The symbol " $\hat{=}$ " means "equal as $x^2 \to 0$" and the index 5 refers to an axial vector current. The local current $I(x)$ and the bilocal currents $I(o|x)$ are defined in the free quark model as

$$I_k(x) \equiv : \bar{\psi}(x)\gamma^\mu \frac{\lambda_k}{2} \psi(x) :$$

$$I_k^{5\mu}(o|x) \equiv : \bar{\psi}(o)\gamma^\mu\gamma^5 \frac{\lambda_k}{2} \psi(x) :$$

As $x_o \to 0$ along the light cone one recovers Gell-Mann's algebra of currents at equal times from the complete set of relations analogous to (15). Fritzsch and Gell-Mann conjecture that this light cone algebra holds in nature independently of the free quark model.

We can now use this algebra to get predictions for the structure functions |13|. Taking the nucleon matrix elements of the two sides of (15) we can write

$$\begin{aligned} &< p,\alpha \mid [\, I_k^{5\sigma}(o|x) + I_k^{5\sigma}(x|o)\,] \mid p,\alpha > \hat{=} \\ &= 2M \{\, \alpha^\sigma \hat{S}_k(p,x) + p^\sigma\, \alpha\cdot x\; i\, \hat{A}_k(p\cdot x) \\ &\quad + x^\sigma\, \alpha\cdot x\; \hat{N}_k(p\cdot x) + O(x^2) \,\} \quad . \end{aligned} \tag{16}$$

Defining fourier transforms by |*|

$$\hat{S}_k(p\cdot x) = \int_{-1}^{1} d\xi\, e^{i\xi p\cdot x}\, S_k(\xi) \text{ etc.}$$

we find in the Bjorken limit (denoted LIM) just

$$\begin{aligned} &\text{LIM } \nu\, X_1(\nu,q^2) = G_1(\omega) = \\ &= -\frac{1}{6}\{\, \frac{1}{\sqrt{3}}\, S_8(\omega^{-1}) + S_3(\omega^{-1}) + 2\sqrt{\tfrac{2}{3}}\, S_o(\omega^{-1}) \end{aligned} \tag{17}$$

|*| The function $\hat{S}_k$, $\hat{A}_k$ and $\hat{N}_k$ are assumed smooth. Then the spectral function in ω^{-1} vanishes for $|\omega^{-1}| \geq 1$, as can be proven using the Jost-Lehmann-Dyson representation for causal commutators.

$$\text{LIM } \nu^2 X_2(\nu,q^2) = G_2(\omega)$$
$$= + \frac{1}{6} \frac{\partial}{\partial(\omega^{-1})} \{ \frac{1}{\sqrt{3}} A_8(\omega^{-1}) + A_3(\omega^{-1}) + 2\sqrt{\frac{2}{3}} A_o(\omega^{-1}) \} \quad (17)$$

We shall not discuss the consequences which can be drawn from the SU(3) structure of these relations for weak and electromagnetic structure functions, but turn at once to the sum rules of interest to us. First we use the property that $A(\omega^{-1})$ vanishes for $|\omega^{-1}| \geq 1$ and assume that it can be integrated. Taking into account the derivative representation for G_2 we obtain (since G_2 is even in ω):

$$2 \int_1^\infty \frac{d\omega}{\omega^2} G_2^{p,n}(\omega) = 0 \quad (18)$$

where the superscript designates a proton or neutron target. This sum rule is consistent with $G_2 \equiv 0$ but does not imply it, since G_2 is not positive definite. The octet members of $I_k^{5\sigma}(o|x)$ are related to $I_k^{5\sigma}(o)$, the axial currents familiar from baryon β-decay. The SU(3) singlet current $I_o^{5\sigma}(o)$ cannot be measured as can the $I_k^{5\sigma}(o)$, $k \neq 0$. We can eliminate it by taking the difference of proton and neutron targets since the singlet current must contribute equally to proton and neutron and so cannot contribute to the difference. This enables us to find a second sum rule -- this time involving G_1. Namely, taking into account that the integral $\int_{-1}^{1} d(\omega^{-1}) S(\omega) \equiv \hat{S}(p\cdot x=0)$ is given by the nucleon matrix element of the local axial vector current, we can easily get

$$2 \int_1^\infty \frac{d\omega}{\omega^2} [G_1^p(\omega) - G_1^n(\omega)] = \frac{1}{3} f_A \quad (19)$$

f_A denotes the β-decay renormalization constant, $f_A = 1.23$. This is equivalent to Bjorken's sum rule for the asymmetry structure functions [18,10] originally derived as a fixed q^2 sum rule. We now are sure that at least one structure function $G_1^{p,n}$ is nonzero. (It would be without meaning to postulate scaling behavior if there were no evidence that the resulting scaling functions did not vanish identically.)

3. Do the above sum rules converge, i.e. was our smoothness assumption correct? It would certainly be useful to have an argument that (18) and (19) are consistent in the sense that the integrals are finite. We can attempt to check this by supposing that the limit $\omega \to \infty$ can be connected to the Regge limit $\nu \to \infty$ |19|. That is, we assume that the leading light cone singularity of the structure functions as $\omega \to \infty$ turns to the leading J-plane singularity in X_i for $\nu \to \infty$ and q^2 large and fixed. The standard Regge folklore gives for fixed q^2

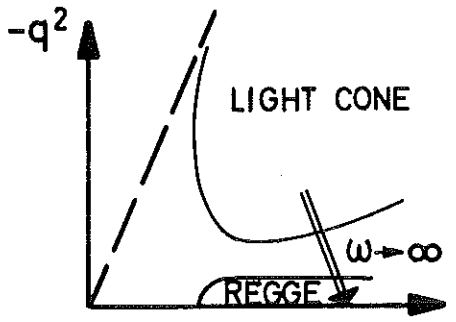

Fig. 5

$$\nu X_1 + \nu^2 X_2 \sim \nu^{\alpha(o)} \tag{20a}$$

$$X_2 \sim \nu^{\alpha'(o)-1} \tag{20b}$$

as $\nu \to \infty$, where $\alpha(o)$ and $\alpha'(o)$ are the intercepts at $t = 0$ of the leading Regge singularities which can contribute to the X_i. The only singularities which can appear are those with unnatural parity, charge conjugation $C = 1$, and signature $\mp$ in (20a,b), respectively. Because of spin conservation in forward scattering, however, X_2 does not have any contributions from factorising Regge singularities (see the Appendix). Hence we are left with cut contributions like $P * f, \ldots$ $\rho * \omega$ etc. with effective intercepts $\alpha'_{eff}(o) \lesssim 1/2$ |*|. The leading contributions to $\nu X_1 + \nu^2 X_2$ come from A_1, $P * A_1, \ldots$ exchange, all expected to have $\alpha_{eff}(o) \lesssim 0$. The correspondence of Regge and light cone behavior which we have assumed leads us to expect:

$$G_1(\omega) + G_2(\omega) \sim \omega^{\alpha_{eff}} \lesssim \text{const} \quad \text{for } \omega \to \infty$$

$$G_2(\omega) \sim \omega^{\alpha'_{eff}+1} \lesssim \omega^{3/2} \quad \text{for } \omega \to \infty$$

We thus see that the sum rule for $G_1 + G_2$ may even converge rather quickly. The case of G_2 is more unclear: the sum rule only converges if the leading $P *$ meson cuts do not couple. On the other hand, this difficutly indicates that the correspondence of Regge and light cone behavior may be doubtful for cut structures.

|*| We do not consider $P * P$ cuts, whatever it may be, having $\alpha_{cut}(o) = 1$.

4. These sum rules provide a rough estimate for the order of magnitude expected for the asymmetry |10|. For $E >> (-q^2)/M$ but $-q^2$ large we have

$$\Delta_{||} \simeq \frac{(-q^2)}{ME} \quad \frac{G_1(\omega) + G_2(\omega)}{F_2(\omega)}$$

From the sum rules (18) and (19) we expect

$$\int_1^\infty d\omega \frac{1}{\omega^2} \left(G_1(\omega) + G_2(\omega) \right) \simeq 0.2$$

for, say, the proton. An estimate for the mean asymmetry is then

$$\frac{ME}{(-q^2)} \langle \Delta_{||} \rangle_\omega \int_1^\infty \frac{d\omega}{\omega^2} F_2(\omega) \simeq 0.2 \qquad (21)$$

and leads us to expect parallel asymmetries of $\sim$ 20 % for E $\sim$ 10 GeV, $-q^2 \sim 2\text{GeV}^2$, averaged over ω.

Finally, we note a curious and amusing consequence of this estimate. The positivity condition (8) can be written as

$$0 \leq \frac{(-q^2)M^2}{\nu^2} \left| \frac{G_1(\omega)}{W_T(\omega)} \right| \leq R(\nu, q^2)$$

the left hand side of which is, given the Bjorken sum rule with G_2 small, ~ 0.2 for not too large $|q^2|$ and E. We thus find two things: first, R cannot vanish faster than $(-q^2)M^2/\nu^2$ and second, in the region where the asymmetries are $\sim$ 20 %, so is R. This is an intriguing connection, but we shall not dwell on it.

IIb. Quark-Parton Models

1. The various parton models |3,4| provide a physical intuitive picture of the inelastic electron-nucleon scattering. In the infinite momentum frame (f.i. the eN center-of-mass as $E \to \infty$) the conditions for the validity of the impulse approximation may be valid. The target nucleon is assumed to behave like a lot of free constituents with bounded transverse momentum, and the interaction time of the photon is vanishingly small compared to the lifetime of this

state. The scattering is then incoherent. If the number of free constituents ("partons" or quarks and gluons) of type j with spin direction σ relative to the nucleon spin and with longitudinal momentum $xP_{||}$ is denoted by $D_{j\sigma}(x)$, one has |4,14|

$$G_1(\omega) = \frac{1}{2} \sum_{j\sigma}{}' D_{j\sigma}(\omega^{-1}) < j\,\sigma \mid Q^2\sigma^3 \mid j\,\sigma > \qquad (22)$$

$$G_2(\omega) = 0$$

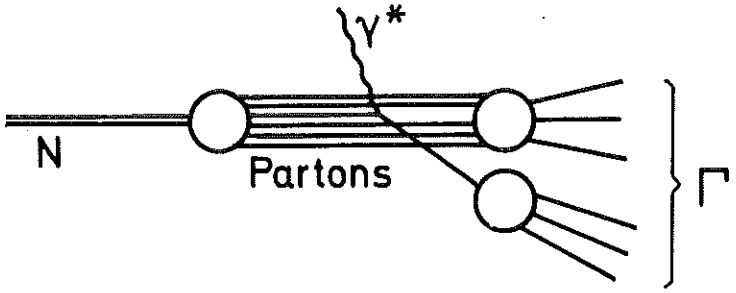

Fig. 6

where the sum runs only over the charged constituents (hence the prime).

An immediate conclusion from (22) is that, perhaps surprisingly, only one of the scaling functions has a nonzero scaling limit. The result $G_2 = 0$ is much stronger than the sum rule (17) from the light cone quark algebra. We make two remarks in this connection:

(i) The result $G_2 = 0$ actually follows from the fact that in the infinite momentum limit point fermions are responsible for the scattering. In this case only one structure function appears for each fermion - the single particle asymmetry function is just that for a free fermion, $A_{\mu\nu}$ in equation (2). Assuming that one can use infinite momentum techniques at all, it is clear that $G_2 = 0$ is a nice test of the idea that the proton constituents behave like pointlike fermions in this limit.

(ii) Taking $G_2 \equiv 0$, the ratio of the absorptive parts of the helicity amplitudes as $\nu \to \infty$ at constant ω is given by

$$\frac{\tau_L}{\tau_T} \sim \frac{\mathrm{Im}\, f^S_{1\ 1/2,0-1/2}}{\mathrm{Im}\, f^S_{1\ 1/2,1\ 1/2} - \mathrm{Im}\, f^S_{1\ 1/2,1\ 1/2}} = -\frac{1}{2}\left[\frac{-2q^2M^2}{\nu^2}\right]^{1/2} \to 0 \qquad (23)$$

This is in conformance with the parton model folklore that those amplitudes with longitudinal photons vanish in the scaling limit relative to those with purely transverse photons. This is not a triviality, since we must have $\nu^2 X_2$ zero in order to get (23).

2. Going further with the quark-parton picture and assuming that any gluons present do not contribute anything to the nucleon spin, we can calculate G_1 for neutron and proton separately. Since the squared charge matrix is $Q^2 = 2/9 + Q/3$ we can use $\int_0^1 d(\omega^{-1}) \sum_{j\sigma} D_{j\sigma}(\omega^{-1}) < j\ \sigma\ |\ \frac{1}{2}\sigma^3|\ j\ \sigma > = 1/2$ (the nucleon spin) and take $<Q\sigma^3>_{j\sigma}$ from the Cabibbo theory of the axial vector baryon currents with the D/F ratio 3/2 to get |14|

$$2\int_1^\infty \frac{d\omega}{\omega^2}\, G_1^p(\omega) = \frac{2}{9} + \frac{f_A}{9}\,\frac{D/F+3}{D/F+1} \simeq 0.47$$

$$2\int_1^\infty \frac{d\omega}{\omega^2}\, G_1^n(\omega) = \frac{2}{9} - \frac{2f_A}{9}\,\frac{D/F}{D/F+1} \simeq 0.06$$

This is a far reaching result: virtually the entire asymmetry effect is confined to $G_1^p(\omega)$, and G_1^n, G_2^p and G_2^n are much smaller. This argument is in the spirit of SU(6) symmetry, and in fact $G_1^n = 0$ would be a consequence of the use of exact SU(6) symmetric baryon wavefunctions, as we shall see.

3. The detailed quark parton model of Kuti and Weisskopf |4| actually gives functional forms for $G_1^{p,n}$, so we turn now to this model. The assumptions are:

(i) Nucleons are made out of three quarks qqq and a sea of $q\bar{q}$ pairs and gluons which have vacuum quantum numbers and are responsible for the diffractive piece of the structure functions. This latter dynamical mess is called the 'core'.

(ii) The single parton distribution functions which are related in the model to the inelastic scattering structure functions are calculated in two steps. First, the authors |4| write down distribution functions for the longitudinal momentum which would hold if the number of core partons, for example, were small. (as in a gas of low density). The final single parton distribution function must take into account the statistical weight of the states where many partons are present, and the requirement that the sum of all fractional longitudinal momenta is unity.

The input distributions are taken to be proportional to longitudinal phase space for the core partons (q or $\bar{q}$), with no transverse momentum, $dP_c \simeq g dx/x$. The gluons satisfy the same expression with a coefficient g'. The "valence" quarks satisfy $dP_v \simeq (x)^{1-\alpha}\, dx/x$, the factor $x^{1-\alpha}$ being necessary to get correct Regge behavior, with $\alpha = \alpha_{A_2}(o) \simeq 1/2$, for the difference $F_2^p - F_2^n$ in the limit $x \to 0$. The constants g and g' are to be obtained at the end by fitting $F_2^p(\omega)$. Using these assumptions,with the Ansätze above for the dP(x) for the whole x-range, the output single quark distribution functions $D_{j\sigma}(x)$ for the valence quarks, core quarks and gluons follow. To get these functions, one has to impose the two steps mentioned above: The multiparton state has to be constructed using the correct statistics and the longitudinal momentum constraint. For details, see the work of Kuti and Weisskopf |4| .

It is worth mentioning the distribution function for the valence quarks,

$$D_v(x) \underset{\sim}{\propto} \frac{\Gamma(6-3\alpha)}{\Gamma(1-\alpha)\,\Gamma(5-2\alpha)}\; x^{-\alpha}\,(1-x)^{4-2\alpha}$$

which dominates as $x \to 1$ |*|. The proportionality coefficient follows from the SU(6) wave function for the 3-quark nucleon state. From all this one gets the structure functions G_1 for proton and neutron as

$$G_1^p(\omega) = \frac{5}{18}\,\frac{\Gamma(6-3\alpha)}{\Gamma(1-\alpha)\,\Gamma(5-2\alpha)}\; x^{-\alpha}\,(1-x)^{4-2\alpha} \qquad (27)$$

$$G_1^n(\omega) = 0$$

The $G_1^{p,n}(\omega)$ obtained in this way obey Bjorken's asymmetry sum rule with the SU(6) value for $f_A = 5/3$.

Obviously, one can only use this for an estimate. There are also some qualitative troubles with the model, namely,
(i) The apparrent experimental violation of $F_2^n/F_2^p \overset{\sim}{\propto} 2/3$ near $\omega = 1$ indicates a strong violation of the simple SU(6) picture for the quark wavefunctions |20| at this point.

|*| Dominance of the valence quarks for $x \to 1$ is one of the weaker points of this model. Following isotropy arguments one would expect the shell quarks to dominate as $x \underset{\sim}{>} 1/3$. The present data analysis strongly supports this suggestion. (Private remark by H. Joos).

One cannot then take $G_1^{n,p}$ too seriously -- at last near $\omega = 1$.
(ii) As $\omega \to \infty$ one has from the model $G_1^p \to \omega^{1/2}$, which is inconsistent with the Regge picture.

IIc. Resonance Models

In concluding our discussion of models, we turn to one due to Domokos et al |7|. The idea here is directly opposite to that behind the parton model, and the results are also wholly different. Domokos et al assume that the nondiffractive part of the deep inelastic scattering is built up by resonances.

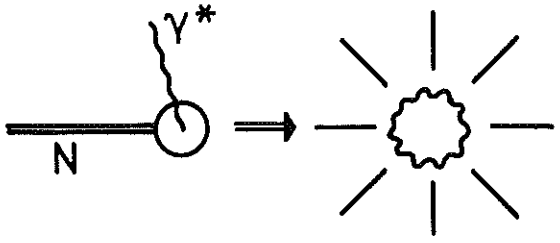

Fig. 7

At low ω one has bumps in the inelastic cross section, which grow progressively smaller as $q^2 \to -\infty$; at higher ω no noticeable bumps exist. The authors conjecture that one is really producing resonances which become progressively smeared out as their mass increases, and that above the familiar resonance region, $W \gtrsim 1.8$ GeV, there are many such broad resonances which collectively build up a smooth scaling function. This is vaguely analogous to the smooth average behavior of scattering amplitudes in nuclear physics problems, which can be built out of many resonance levels (compound nucleus model).

In order to implement this idea one needs assumptions about the resonance spectrum and the transition form factors. Rather than discuss these rather speculative assumptions in detail, we refer the reader to the original papers. To summarize briefly,
(i) the authors assume that the resonance spectrum is that of a harmonic oscillator, $M_n^2 = m_N^2(1+n)$ with spins $j = 1/2, 3/2, \ldots n + 1/2$ and normality $\tau = \pm$. The levels with even n have isospin 1/2 and those with odd n have isospin 3/2.
(ii) the relative weight of the photon-nucleon decay channel is inversely proportional to the resonance mass.

(iii) The transition form factors for each isospin channel are universal functions of $q^2/M_n^2 = y$ with the following dipole form for $q^2 \to -\infty$:

$$I = 1/2: \hat{G}_1 = G_E = Q(1-r^2y)^{-2}; \hat{G}_2 = 0; \hat{G}_3 = G_M = \mu_{1/2}(1-r^2y)^{-2} \qquad (24)$$

$$I = 3/2: \hat{G}_1 = Q(1-r^2y)^{-2}; \hat{G}_2 = \hat{G}_3; \hat{G}_3 = \mu_{3/2}(1-r^2y)^{-2}$$

where the parameters are taken from the nucleon and first resonances:

$$r^2 \simeq \sqrt{2} \qquad \mu_{1/2} \simeq \begin{cases} \mu_p \\ \mu_n \end{cases} \qquad \mu_{3/2} \simeq \begin{cases} +\mu_p & \text{proton target} \\ -\mu_p & \text{neutron target} \end{cases}$$

The precise definition of the functions G_i can be found in the original papers; we only want to exhibit their functional form.

We want to emphasize that introduction of the poorly understood scale variable y into the form factors is crucial in "deriving" scale invariance of the deep inelastic structure functions in ω.

The model gives R = 0; it provides good agreement with the functional form of F_2. This agreement rests heavily on assumptions (ii) and (iii). The calculation of the polarization structure functions [16] yields two surprises when compared to the quark parton model and the light cone algebra. First, $G_1(\omega)$ is nearly zero,

$$G_1^p(\omega) \simeq G_1^n(\omega) \simeq 0 \qquad (25)$$

and second, $G_2^{p,n}$ takes the following values

$$G_2^{p,n}(\omega) \sim \frac{\omega(\omega-1)^3}{(\omega-1+\frac{r}{2})^4} \left\{ \frac{\mu^2_{\hat{p},n}}{2} - \frac{\mu^2_{3/2}(\omega-1)}{(1+\frac{r}{2})\,\omega-1} \right\} \text{ for } \omega \to 1 \text{ and } \infty \qquad (26)$$

there being no significant n-p difference as in the quark parton model. The authors point out that these results are sensitively dependent on the transition form factors: Whereas $\nu W_2(\nu,q^2)$ is built up out of the sum of the squared form factors of the resonances, $\nu^2 X_2(\nu,q^2)$ is related to the differences of

squares. As specific example of the sensitivity of the model predictions to the input, 10% changes in the I = 3/2 assumption $\hat{G}_2 = \hat{G}_3$ lead to drastic changes in the asymmetries, as can be seen from the figures at the end of this report |16|.

III. Summary

We conclude this report by collecting what we have done into some simple statements. The spin averaged structure functions F_1 and F_2 are model dependent, but only weakly so. We can expect in the near future that several theories of deep inelastic scattering will give satisfactory accounts of F_1 and F_2 with possibly very different underlying physical ideas. These ideas will have different consequences for more involved reactions like $e + N \to e' + \pi +$ anything. It's likely, however, that in order to decisively test the theories of deep inelastic scattering one will have to measure the spin dependent structure functions G_1 and G_2. Because of the Bjorken asymmetry sum rule, even a negative result - asymmetries far under 20 % - would have far - reaching consequences.

An experimental program to measure asymmetries must concentrate, if at all possible, on separating G_1 and G_2. At low energies, the measurement of asymmetries in the "near" deep inelastic region (1.8 GeV $\lesssim$ W $\lesssim$ 3.0 GeV; 0.3 GeV^2 $\lesssim$ $|q^2|$ $\lesssim$ 1.5 GeV^2) is obviously connected to the question of how the asymmetries allow to understand the transition to the assumed scaling behavior. This region is particularly appropriate to tests of resonance models for the scaling functions F_1, F_2, G_1 and G_2. At high energies, in the "far" deep inelastic region, one can test how well scaling for G_1 and G_2 is fulfilled. If scaling holds, one should then attempt to obtain the functional forms of G_1 and G_2 so as to give accurate tests of the sum rules. In particular, one would like to know whether the neutron shows any asymmetry effects, and whether $G_2^{p,n} \simeq 0$ or not.

We close with a table showing the predictions of the different models.

	Light cone algebra	Quark-Parton Model	Resonance Model
$G_1(\omega)$ Proton Neutron	$\int_1^\infty \frac{d\omega}{\omega^2}[G_1^p - G_1^n] = \frac{f_A}{6}$	$G_1^p(\omega) \sim \omega^{+1/2}(1-\omega^{-1})^3$ $G_1^n(\omega) = 0$	$G_1^p(\omega) \simeq 0$ $G_1^n(\omega) \simeq 0$
$G_2(\omega)$ Proton Neutron	$\int_\omega^\infty \frac{d\omega}{\omega^2} G_2^{p,n}(\omega) = 0$	$G_2^p(\omega) = 0$ $G_2^n(\omega) = 0$	$G_2^{p,n}(\omega) \sim F(\omega)\left[\frac{\mu_{p,n}^2}{2} - \frac{\mu_{3/2}^2(\omega-1)}{(1+\frac{r}{2})\omega-1}\right]$ $F(\omega) \sim \frac{\omega(\omega-1)^3}{(\omega-1+\frac{r}{2})^4}$

Figs. 8a - 8l:

In this first series of figures, we show the supper limits to the parallel and perpendicular asymmetries for energies E = 5 GeV (DESY), 15 GeV (SLAC), 50 GeV, 100 GeV(CERN II and Batavia) at lepton scattering angles $\theta = 10^{\circ}$, 20° and 30°. The parallel asymmetry $\Delta_{||}$ refers to the case where the nucleon spin and the lepton spin (necessarily along the lepton flight direction) are parallel. The perpendicular asymmetry refers to the case where the nucleon spin is in the scattering plane and perpendicular to the lepton spin direction. The bounds on $\Delta_{\perp}$ and $\Delta_{||}$ come from the positivity constraints on the deep inelastic structure functions. The partial suppression of $|\Delta_{\perp}|$ relative to $|\Delta_{||}|$ arises from the kinematical factor $\sim \sin\theta$ in front of $|\Delta_{||}|$ and the choice of small θ (necessary for reasonable counting rates). We have chosen in the first figures $R = \sigma_L/\sigma_T = \cdot 18$; decreasing R toward zero has little effect on $|\Delta_{||}|$, but it can decrease $|\Delta_{\perp}|$ drastically. This dependence is shown in the last figure at each energy.

Figs. 9a - 9h:

In this second series, we present the detailed predictions of the Kuti-Weisskopf quark-parton model for the parallel and perpendicular asymmetries for a proton target at the same lepton energies and scattering angles as above. The neutron asymmetries vanish in this model. The model presumably involves uncertainties of at least $\simeq$ 30 %, and cannot be taken literally for $\omega \simeq 1$. The suppression of $\Delta_{\perp}$ is partially kinematical in origin. The parallel asymmetry $\Delta_{||}$ does not vary too much as a function of E, having a mean value $\sim$ 20 %. The perpendicular asymmetry is $\sim$ 1 % for all energies. Note that the model has R set equal to zero.

Fig. 10:

Here we show, for comparison, the parallel asymmetry predicted by the resonance model of Domokos, Domokos-Kövesi and Schonberg. The curves are independent of lepton energy an scattering angle. The full curve corresponds to the symmetric quark model and the dashed curve to a 10 % symmetry breaking.

Appendix

The purpose of this Appendix is to present the relations between our X_i and the corresponding invariants due to other authors |*|; to give the s- and t-channel helicity amplitudes; and to give a brief discussion of the Regge behavior of the X_i. Our metric is $g_{oo} = +1$, $g_{ii} = -1$, $i = 1,2,3$. We also use Bjorken and Drells' conventions (e.q. $\varepsilon_{0123} = +1$) in their field theory textbooks.

We have defined the tensor $X^{\mu\nu}$ as

$$X^{\mu\nu} = \varepsilon^{\mu\nu\rho\sigma} q_\rho \alpha_\sigma X_1(\nu,q^2) + (\alpha\cdot q)\varepsilon^{\mu\nu\rho\sigma} q_\rho p_\sigma X_2(\nu,q^2) \qquad (A.1)$$

as has Wray |13|.

Bjorken |10| defined

$$\begin{aligned} X^{\mu\nu} = {} & [p^\nu \varepsilon^{\mu\rho\sigma\tau} p_\rho \alpha_\sigma q_\tau - p^\mu \varepsilon^{\nu\rho\sigma\tau} p_\rho \alpha_\sigma q_\tau - (p\cdot q)\varepsilon^{\mu\nu\rho\sigma} p_\rho \alpha_\sigma] \; H_1(\nu,q^2) \\ & + [q^\nu \varepsilon^{\mu\rho\sigma\tau} p_\rho \alpha_\sigma q_\tau - q^\mu \varepsilon^{\nu\rho\sigma\tau} p_\rho \alpha_\sigma q_\tau - q^2 \varepsilon^{\mu\nu\rho\sigma} p_\rho \alpha_\sigma] \; H_2(\nu,q^2) \end{aligned} \qquad (A.2)$$

and Gourdin |14| has

$$\begin{aligned} X^{\mu\nu} = {} & \varepsilon^{\mu\nu\rho\sigma} q_\rho \alpha_\sigma \; Y_1(\nu,q^2) \\ & + (n^\mu P^\nu - n^\nu P^\mu) \; Y_2(\nu,q^2) \end{aligned} \qquad (A.3)$$

where

$$n^\mu = \varepsilon^{\mu\rho\sigma\tau} p_\rho \alpha_\sigma q_\tau$$

$$P^\mu = p^\mu - \frac{p\cdot q}{q^2} q^\mu \quad .$$

The relations between these other functions and ours are

|*| The reader should check for extra overall factors in these definitions. We have defined all invariants with respect to our normalization convention, not those of the original authors.

$$H_1 = -\frac{1}{M^2}\ (X_1 + \nu X_2)$$
$$H_2 = X_2 \qquad (A.2')$$

$$Y_1 = X_1 + \left(1 - \frac{M^2 q^2}{\nu^2}\right) \nu X_2$$
$$Y_2 = -\frac{q^2}{\nu}\ X_2 \qquad (A.3')$$

The independent s-channel helicity amplitudes for off-shell forward Compton scattering are

$$f^S_{1\pm1/2;\ 1\pm1/2} = T_1 \pm [\nu T_3 + (\nu^2 - M^2 q^2)\ T_4]$$
$$f^S_{o\ 1/2;o\ 1/2} = -T_1 + \left(M^2 - \frac{\nu^2}{q^2}\right) T_2 \qquad (A.4)$$
$$f^S_{1\ 1/2;0-1/2} = +(-2q^2M^2)^{1/2}\ T_3$$

with photon helicity wave functions

$$\varepsilon^\mu(\pm 1) = \mp\ \frac{1}{\sqrt{2}}\ (0, 1, \pm i, 0)$$

$$\varepsilon^\mu(o) = \frac{1}{\sqrt{-q^2}}\ (|\vec{q}|, 0, 0, q^o)$$

the first of which is a spacelike, the second a timelike vector. The W_i and X_i are the absorptive parts of the full Comtpon amplitudes defined above,

$$W_{1,2} = Im\ T_{1,2}$$
$$X_{1,2} = Im\ T_{3,4} \qquad (A.5)$$

with the $Im\ f^S_{\{\lambda\}}$ similarly defined.

We obtained the t-channel helicity amplitudes from those in the s-channel by using the s-t crossing matrix. The elements of the matrix are simply numbers at $t = 0$, and we find

$$f^t_{1/2\ 1/2;11} = \frac{1}{4}\left(f^S_{1\ 1/2;\ 1\ 1/2} + f^S_{1-1/2;1-1/2}\right) + \frac{1}{2} f^S_{o1/2;o1/2} + \frac{1}{\sqrt{2}} f^S_{1\ 1/2;o-1/2}$$

$$= \frac{1}{2}\left(M^2 - \frac{\nu^2}{q^2}\right) T_2 + \sqrt{-M^2q^2}\ T_3$$

$$f^t_{1/2\ 1/2;1-1} = \frac{1}{4}\left(f^s_{1\ 1/2;1\ 1/2} + f^s_{1-1/2;1-1/2}\right) - \frac{1}{2} f_{o1/2;o1/2}$$

$$= T_1 - \frac{1}{2}\left(M^2 - \frac{\nu^2}{q^2}\right) T_2$$

$$f^t_{1/2\ 1/2;oo} = \frac{1}{2}\left(f^s_{1\ 1/2;1\ 1/2} + f^s_{1-1/2;1-1/2}\right) \qquad (A.6)$$

$$= T_1$$

$$f^t_{1/2-1/2;o1} = \frac{1}{2\sqrt{2}}\left(f^s_{1\ 1/2;1\ 1/2} - f^s_{1-1/2;1-1/2}\right) - \frac{1}{2} f^s_{1\ 1/2;o-1/2}$$

$$= \frac{1}{\sqrt{2}}\left[\left(\nu - \sqrt{-M^2q^2}\right) T_3 + \left(\nu^2 - M^2q^2\right) T_4\right]$$

We are interested in T_3 and T_4; the asymptotic behavior, ignoring here T_1 and T_2, is

$$f^t_{1/2\ 1/2;11} \overset{\nu}{\sim} \text{const}\ T_3$$

$$f^t_{1/2-1/2,01} \to \text{const}\ \left(\nu\ T_3 + \nu^2 T_4\right) \qquad (A.7)$$

at fixed q^2, for $\nu \to \infty$. We thus have definite Regge behavior for T_3 and a special linear combination of T_3 and T_4. The former is even under crossing ($\nu \to -\nu$) and recieves contributions from even signature singularities. The latter is odd under ($\nu \to -\nu$) and corresponds to odd signature. We call these α_e and α_o,

$$T_3 = \sum_{\alpha_e} \beta_e \frac{1+e^{i\pi\alpha_e}}{\sin \pi\alpha_e} \left(\frac{\nu}{\nu_o} \right)^{\alpha_e}$$

$$\nu T_3 + \nu^2 T_4 = \sum_{\alpha_o} \beta_o \frac{1-e^{i\pi\alpha_o}}{\sin\pi\alpha_o} \left(\frac{\nu}{\nu_o} \right)^{\alpha_o} . \qquad \text{(A.8)}$$

Additional log ν factors from cuts are not indicated.

The $N\bar{N}$ system in the t-channel has two kinds of states which can annihilate into two photons: Those with parity = $(-)^J$, where J is the total angular momentum in the t-channel, and those states with parity = $(-)^{J+1}$. Only the latter can couple to the fully antisymmetric Levi-Civita tensor $\varepsilon^{\mu\nu\rho\sigma}$.

Acknowledgment:

We should like to thank J. K. Bienlein and R. J. Krisciokaitis for useful discussions about the problems involved in polarization measurements. Furthermore we acknowledge discussions in a DESY seminar where this review has been presented. In particular, we are very grateful to H. Joos for valuable suggestions concerning the models considered. We are much indebted to B. Renner for a critical reading of the manuscript. One of us (P.Z.) expresses his gratitude to H. Joos, E. Lohrmann and W. Paul for the hospitality extended to him at DESY.

References:

|1| J.D. Bjorken, Phys. Rev. 179 (1969) 1547.

|2| H.W. Kendall, Proc. of the International Symposium on Electron and Photon Interactions at High Energies, Cornell University, Ithaca, August 1971.

|3| R. Feynman, Phys. Rev. Letters 23 (1969) 1415.
J.D. Bjorken and E.A. Paschos, Phys. Rev. 185 (1969) 1975.
S.D. Drell, D.J. Levy and T.M. Yan, Phys.Rev. 187 (1969) 2159 etc.

|4| J. Kuti and V.F. Weisskopf, Phys. Rev. D 4 (1971) 3418

|5| C.H.L. Smith, Parton Models of Inelastic Lepton Scattering, International Summer Institute in Theoretical Physics, DESY Hamburg, July 1971.

|6| H.D. Dahmen, Theorie der tiefinelastischen Lepton-Streuung, Vorlesungsnotizen der Herbstschule Maria-Laach, Sept. 1971.

|7| G. Domokos, S. Kovesi-Domokos and E. Schonberg, Phys. Rev. D 3 (1971) 1184.

|8| Y. Frishman, Phys. Rev. Letters 25 (1970) 966.
R. Brandt and G. Preparata, Nucl. Phys. B 27 (1971) 541

|9| H. Fritzsch and M. Gell-Mann in the Proceedings of the Coral Gables Conference on Fundamental Interactions at High Energy, 1971.
J.M. Cornwall and R. Jackiw, Phys. Rev. D 4 (1971) 367.
D.J. Gross and S.B. Treiman, Phys. Rev. D 4 (1971) 1059.

|10| J.D. Bjorken, Phys. Rev. D 1 (1970) 1376.

|11| L. Gálfi, J. Kuti and A. Patkós, Phys. Letters 31 B (1970) 465.
L. Gálfi, P. Gnädig, J. Kuti, F. Niedermayer and A. Patkós, Deep Inelastic Scattering of Polarized Beam from Polarized Nucleon Target, Preprint Budapest, 1970.
M.G. Doncel and E.D. de Raffael, Nuov.Cim. 4 A (1971) 363.

|12| Y. Georgelin, J. Stern and J. Jersak, Nucl. Phys. B27 (1971) 493.

|13| D. Wray, Polarisation in Deep Inelastic Scattering from the Light Cone Quark Algebra, Weizmann Institute, WIS 71/47 Ph.

|14| M. Gourdin, Nucl. Phys. B 38 (1972)418.

|15| Nash, Nucl. Phys. B 31 (1971) 419.
A.J.G. Hey and J.E. Mandula, Light Cone Analysis of Spin Dependent Deep Inelastic Electron Scattering, Caltech Pasadena Preprint, CALT-68-342, 1972.

|16| G. Domokos, S. Kovesi-Domokos and E. Schonberg, Phys.Rev. D 3(1971)1191.

|17| J. Kuti, Deep Inelastic Scattering of Polarized Leptons from Polarized Nucleons, IInd International Conference on Polarized Targets, Berkeley, 1971.

|18| J.D. Bjorken, Phys. Rev. 148 (1966) 1467.

|19| H.D.I. Abarbanel, M.L. Goldberger and S.B. Treiman, Phys.Rev. Letters 22 (1969) 500.
H. Harari, Phys. Rev. Letters 22 (1969) 1078.

|20| H. Fritzsch and M. Gell-Mann, Light Cone Current Algebra, Proc. of the Int. Conf. on Duality and Symmetry in Hadron Physics, Tel Aviv 1971 (The Weizmann Science Press of Israel) 317.

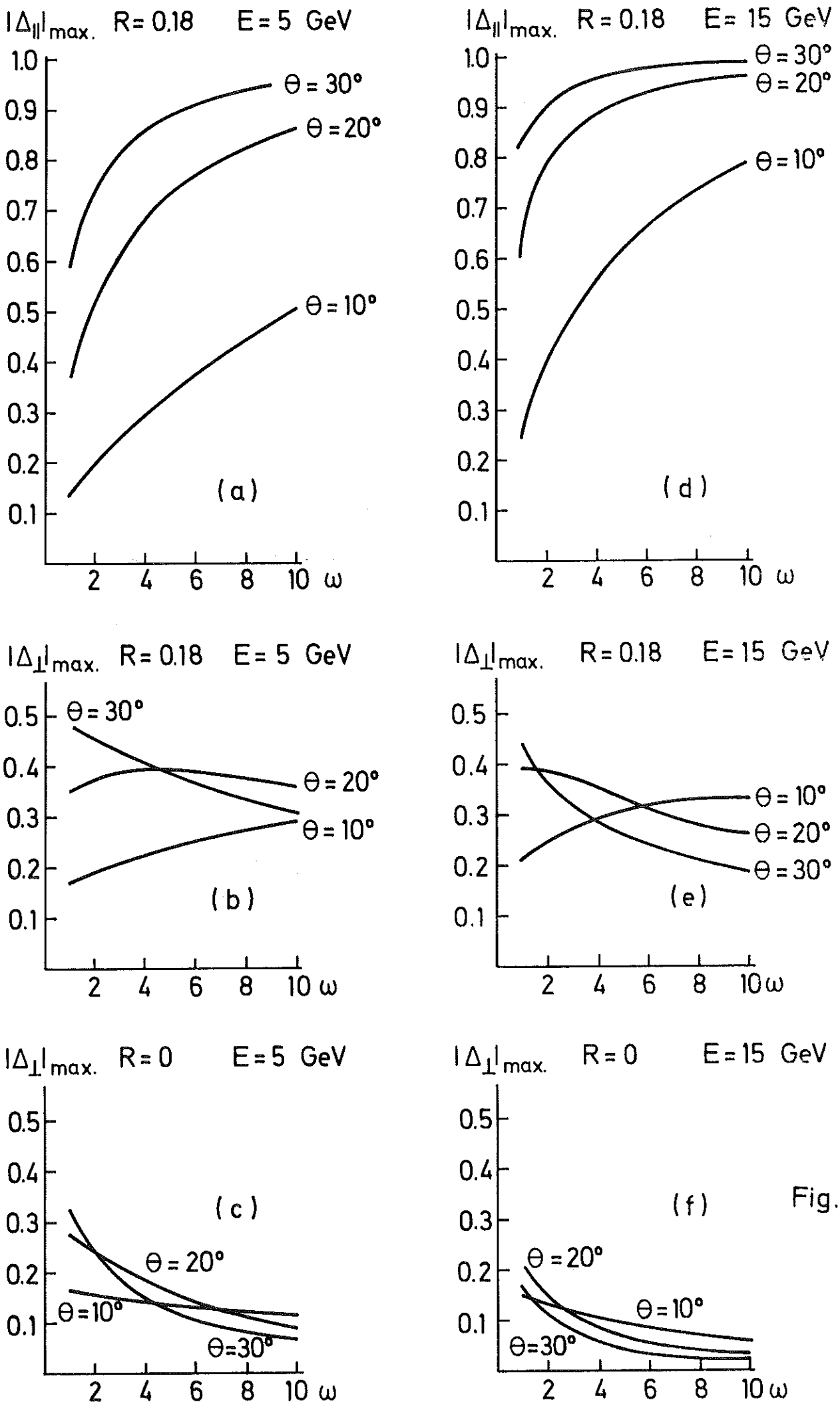
$|\Delta_{\parallel}|_{max.}$ R = 0.18 E = 5 GeV
Θ = 30°
Θ = 20°
Θ = 10°
(a)
$|\Delta_{\parallel}|_{max.}$ R = 0.18 E = 15 GeV
Θ = 30°
Θ = 20°
Θ = 10°
(d)
$|\Delta_{\perp}|_{max.}$ R = 0.18 E = 5 GeV
Θ = 30°
Θ = 20°
Θ = 10°
(b)
$|\Delta_{\perp}|_{max.}$ R = 0.18 E = 15 GeV
Θ = 10°
Θ = 20°
Θ = 30°
(e)
$|\Delta_{\perp}|_{max.}$ R = 0 E = 5 GeV
Θ = 20°
Θ = 10°
Θ = 30°
(c)
$|\Delta_{\perp}|_{max.}$ R = 0 E = 15 GeV
Θ = 20°
Θ = 10°
Θ = 30°
(f)
ω

Fig. 8

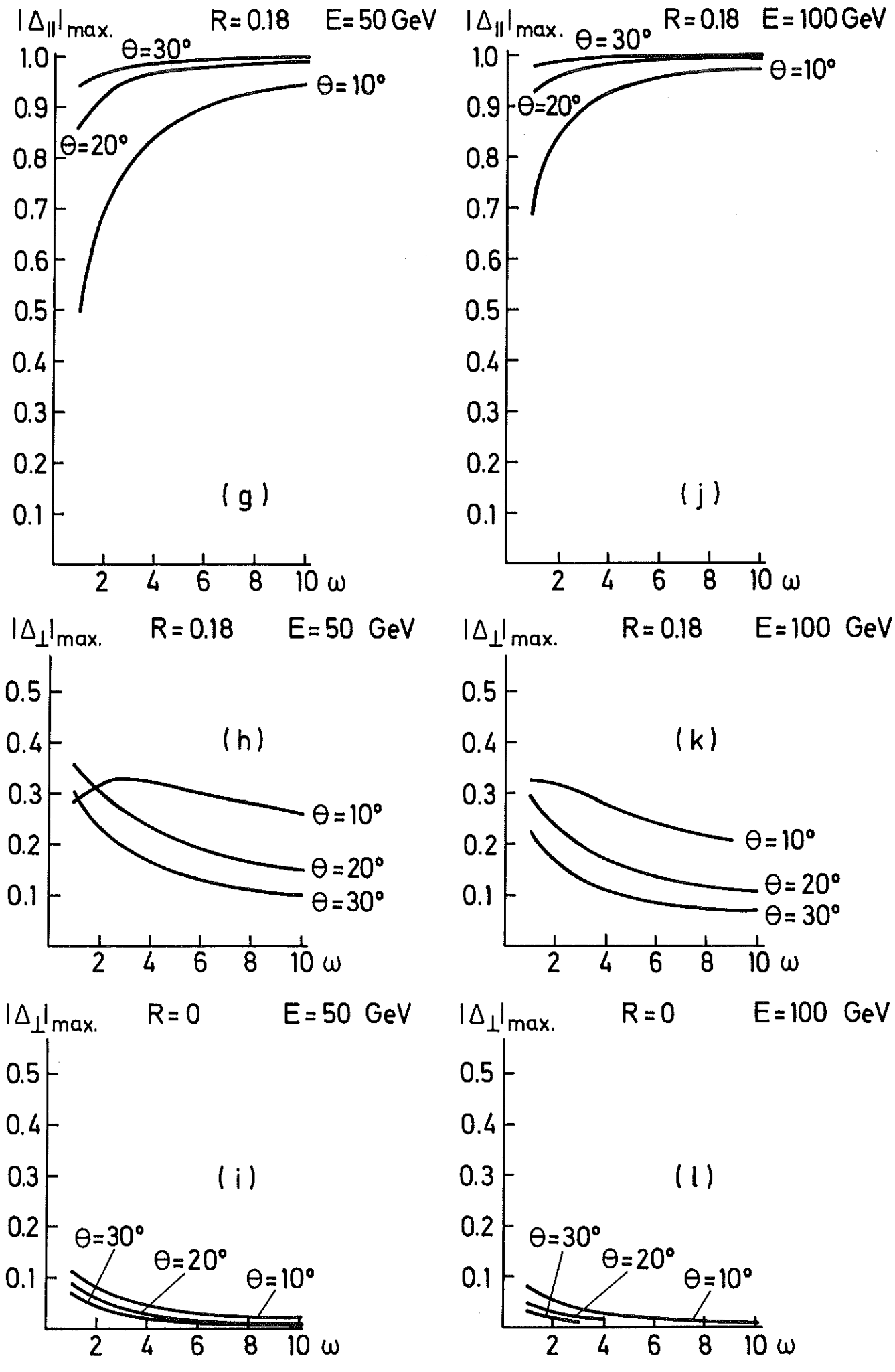
$|\Delta_{\parallel}|_{max.}$
R = 0.18
E = 50 GeV
Θ=30°
Θ=10°
Θ=20°
1.0
0.9
0.8
0.7
0.6
0.5
0.4
0.3
0.2
0.1
(g)
2 4 6 8 10 ω
$|\Delta_{\parallel}|_{max.}$
R = 0.18
E = 100 GeV
Θ=30°
Θ=10°
Θ=20°
(j)
$|\Delta_{\perp}|_{max.}$
R = 0.18
E = 50 GeV
0.5
0.4
0.3
0.2
0.1
(h)
Θ=10°
Θ=20°
Θ=30°
2 4 6 8 10 ω
$|\Delta_{\perp}|_{max.}$
R = 0.18
E = 100 GeV
(k)
Θ=10°
Θ=20°
Θ=30°
$|\Delta_{\perp}|_{max.}$
R = 0
E = 50 GeV
(i)
Θ=30°
Θ=20°
Θ=10°
$|\Delta_{\perp}|_{max.}$
R = 0
E = 100 GeV
(l)
Θ=30°
Θ=20°
Θ=10°

Fig. 8

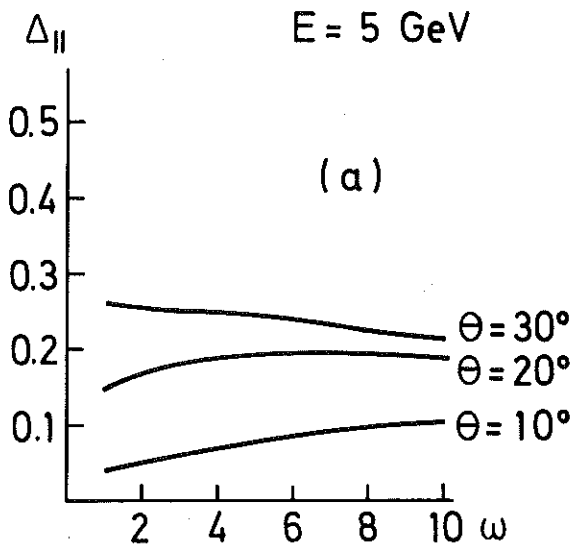
$\Delta_{\parallel}$
E = 5 GeV
(a)
0.5
0.4
0.3
0.2
0.1
Θ = 30°
Θ = 20°
Θ = 10°
2 4 6 8 10 ω

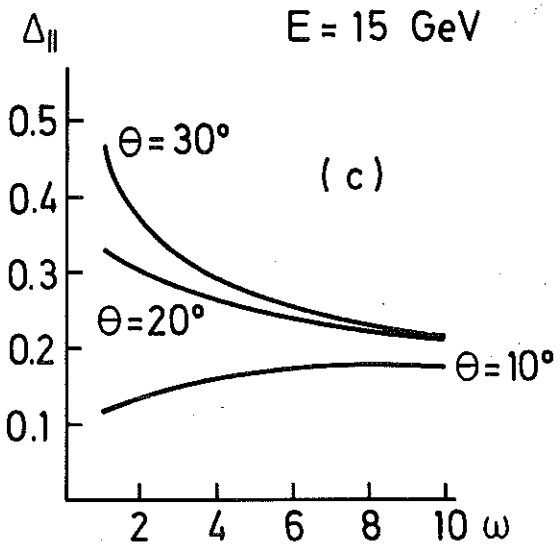
$\Delta_{\parallel}$
E = 15 GeV
(c)
0.5
0.4
0.3
0.2
0.1
Θ = 30°
Θ = 20°
Θ = 10°
2 4 6 8 10 ω

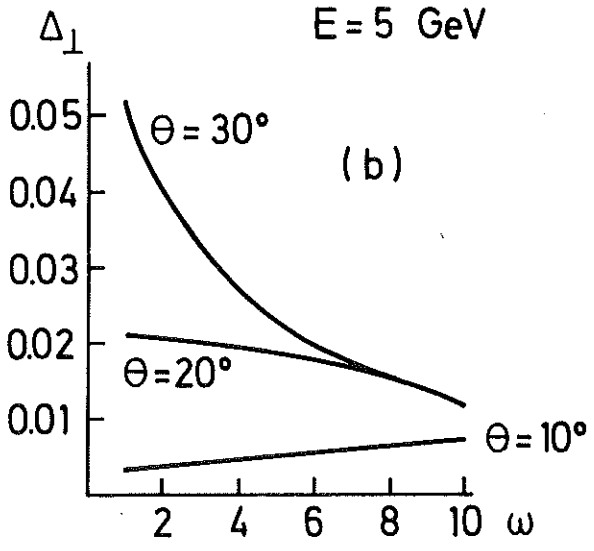
$\Delta_{\perp}$
E = 5 GeV
(b)
0.05
0.04
0.03
0.02
0.01
Θ = 30°
Θ = 20°
Θ = 10°
2 4 6 8 10 ω

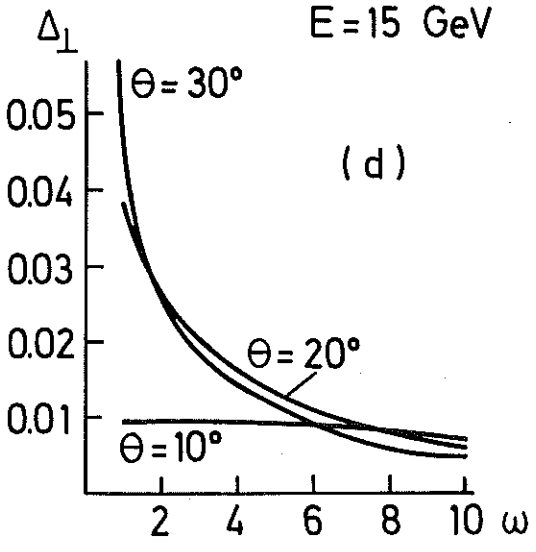
$\Delta_{\perp}$
E = 15 GeV
(d)
0.05
0.04
0.03
0.02
0.01
Θ = 30°
Θ = 20°
Θ = 10°
2 4 6 8 10 ω

Fig. 9

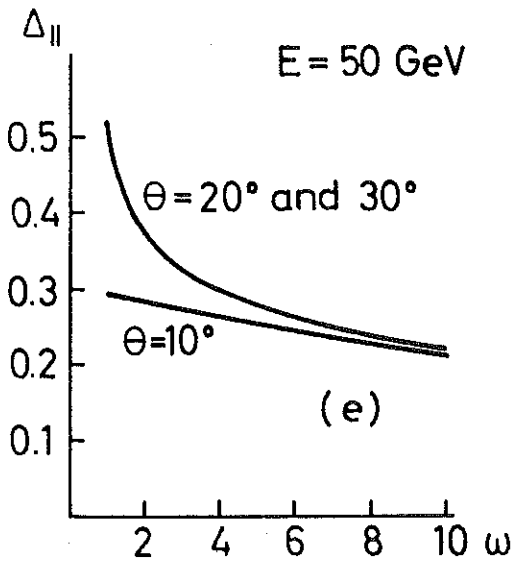
$\Delta_{\parallel}$
E = 50 GeV
0.5
0.4
0.3
0.2
0.1
θ = 20° and 30°
θ=10°
(e)
2
4
6
8
10 ω

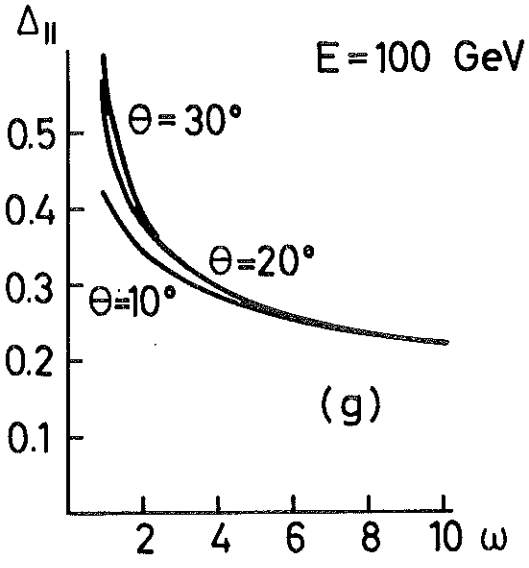
$\Delta_{\parallel}$
E = 100 GeV
0.5
0.4
0.3
0.2
0.1
θ = 30°
θ=20°
θ=10°
(g)
2
4
6
8
10 ω

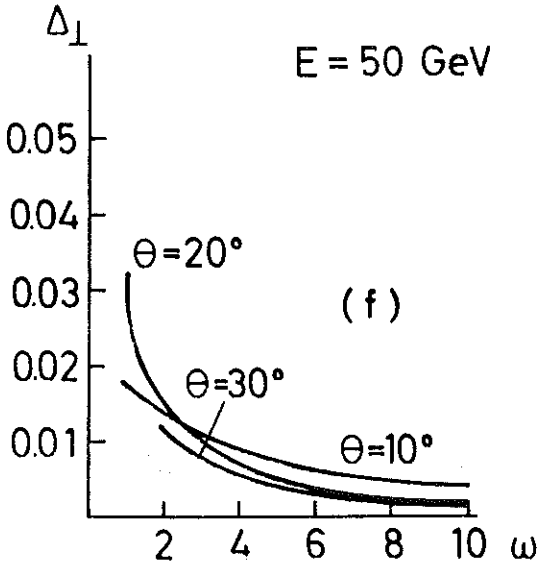
$\Delta_{\perp}$
E = 50 GeV
0.05
0.04
0.03
0.02
0.01
θ=20°
(f)
θ=30°
θ=10°
2
4
6
8
10 ω

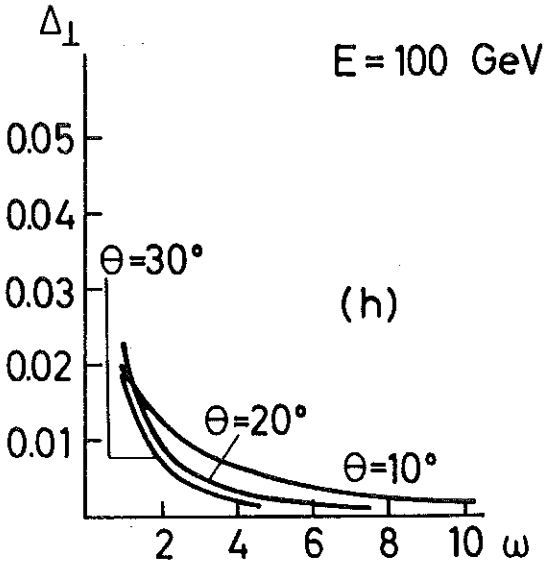
$\Delta_{\perp}$
E = 100 GeV
0.05
0.04
0.03
0.02
0.01
θ=30°
(h)
θ=20°
θ=10°
2
4
6
8
10 ω

Fig. 9

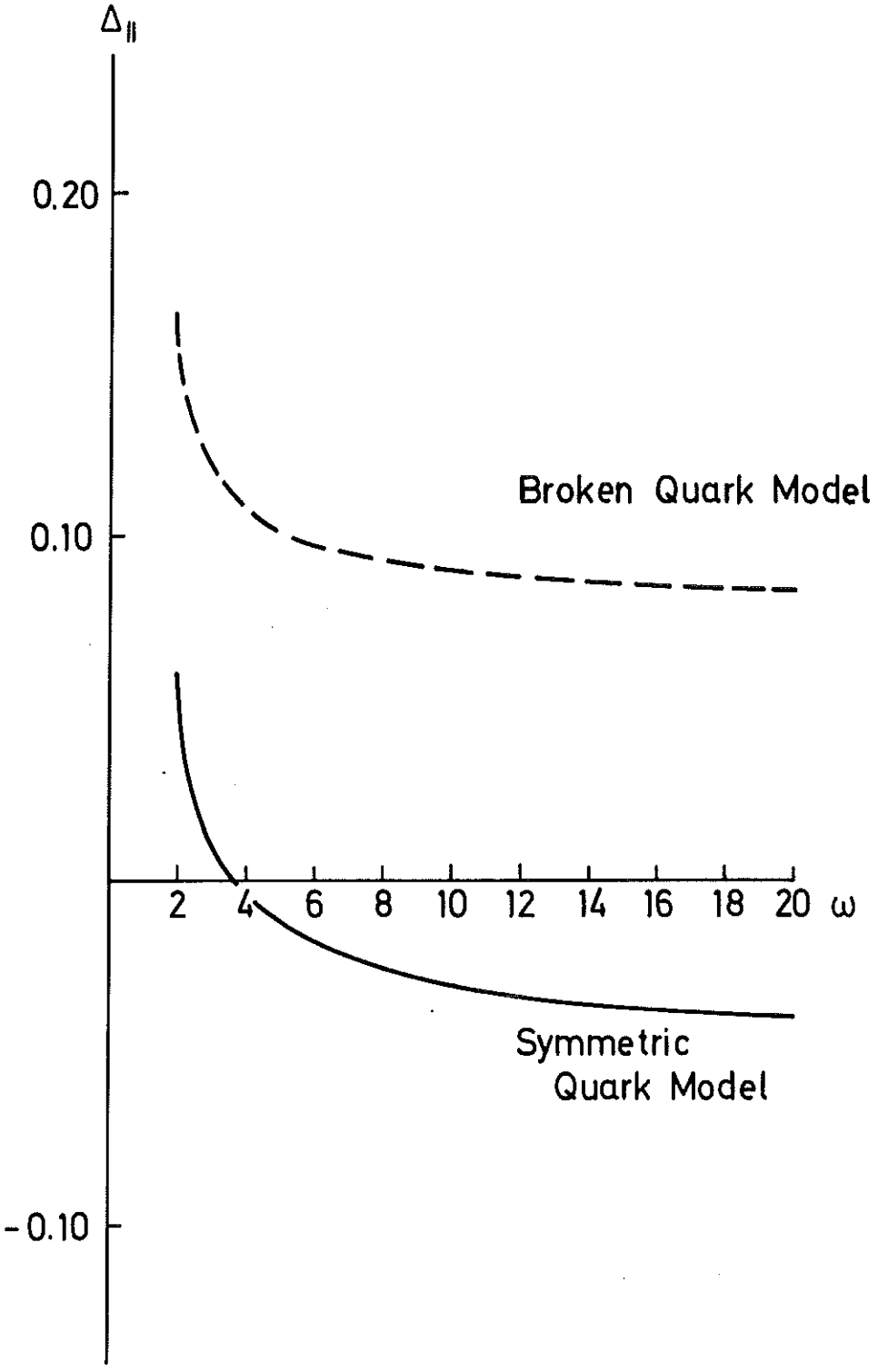
Δ_{II}
0.20
0.10
-0.10
2
4
6
8
10
12
14
16
18
20
ω
Broken Quark Model
Symmetric
Quark Model

Fig. 10